Acta Scientiarum
http://periodicos.uem.br/ojs
ISSN on-line: 1807-8621
https://doi.org/10.4025/actasciagron.v48i1.74683

Expression of apomixis genes during reproductive development in *Urochloa decumbens* and *Urochloa ruziziensis* (Poaceae)

Mara Jane da Rocha[1], Ana Gabriela Damasceno[1], Rubens Diogo Junior[2], Heloisa Oliveira dos Santos[2], Fausto Souza Sobrinho[3], Vânia Helena Techio[1] and Welison Andrade Pereira[1*]

[1]Departamento de Biologia, Universidade Federal de Lavras, Av. Central, s/n, Campus Universitário, 37200-000, Lavras, Minas Gerais, Brazil. [2]Departamento de Agricultura, Universidade Federal de Lavras, Lavras, Minas Gerais, Brazil. [3]Empresa Brasileira de Pesquisa Agropecuária, Embrapa Gado de Leite, Juiz de Fora, Minas Gerais, Brazil. *Author for correspondence. E-mail: welison.pereira@ufla.br

ABSTRACT. This study aimed to correlate the developmental stages of the embryo sac with the morphometric traits of spikelets and to characterize the expression of the *BbrizRan*, *BbrizSti1*, and *BbrizAGL6* genes in *Urochloa ruziziensis* (sexual) and *U. decumbens* (apomictic). Data on the length and diameter of spikelets and anatomical sections were also obtained. Gene expression was determined using RT-qPCR in spikelets at megasporogenesis and megagametogenesis. The spikelet length could be used as a reliable morphological marker to discriminate between the two stages in both species. The embryo sacs observed were of the *Polygonum* type in *U. ruziziensis* and the *Panicum* type in *U. decumbens*. RT-qPCR analysis revealed that the *BbrizRan*, *BbrizSti1*, and *BbrizAGL6* genes were differentially expressed in the studied species during reproductive development. The *BbrizSti1* gene was more highly expressed in *U. decumbens* (apomictic) than in *U. ruziziensis* (sexual) during megasporogenesis, while for *BbrizRan*, *U. decumbens* showed higher expression than *U. ruziziensis* during both megasporogenesis and megagametogenesis. An increase in the expression level of *BbrizAGL6* was observed in both species at both developmental stages of the embryo sac.

Keywords: *Brachiaria*; gene expression; apomixis; megasporogenesis; megagametogenesis.

Received on November 14, 2024.
Accepted on April 16, 2025.

Introduction

Urochloa P. Beauv. (syn. *Brachiaria* (Trin.) Griseb.) is the most important genus of forage grasses used in pastures in tropical countries (Jank et al., 2014; Ferreira et al., 2021). *Urochloa ruziziensis* (R. Germ. & C.M. Evrard) Morrone & Zuloaga, *U. decumbens* (Stapf) RD Webster, and *U. brizantha* (Hochst. Ex A. Rich.) RD Webster form an agamic complex (Lutts et al., 1991; Renvoize et al., 1996). *Urochloa ruziziensis* (2n = 2x = 18) exhibits sexual reproduction (Valle et al., 2001), and after polyploidy induction (Ishigaki et al., 2009; Timbó et al., 2014), it is used as a female parent in crosses with the apomictic *U. decumbens* and *U. brizantha* (both 2n = 4x = 26) (Valle & Pagliarini, 2009).

The transfer of apomixis to sexual species can reduce breeding costs and time due to the faster production of stable superior genotypes (Cruz et al., 1998). In addition, it can facilitate commercial hybrid production since the apomictic hybrid can be multiplied over generations without the loss of vigor or genotype variations (Hanna & Bashaw, 1987; Cruz et al., 1998; Sailer et al., 2016).

Segregation analyses show that the genetic inheritance of apomixis in *Urochloa* is dominant and linked to a single gene locus (Valle & Savidan, 1996; Valle et al., 2001; Zorzatto et al., 2010), which might favor manipulation by genetic engineering. For this reason, studies have been done to identify differentially expressed genes in the embryo sac at different developmental stages between genotypes with different modes of reproduction in *Poa pratensis* L. (Albertini et al., 2004), *U. brizantha* (Rodrigues et al., 2003; Silveira et al., 2012; Guimarães et al., 2013; Lacerda et al., 2013), and *Pennisetum ciliare* (L.) Link (Sing et al., 2007), determining genes and mechanisms potentially associated with apomixis.

In *U. brizantha*, Rodrigues et al. (2003) identified cDNA sequences differentially expressed in the ovaries of sexual and apomictic plants using differential-display PCR and a northern blot. Alves et al. (2007) analyzed the expression of cDNA sequences *BbrizMYO*, *BbrizAQP*, and *BbrizMAP*, encoding a myosin, an aquaporin, and a mitogen-activated protein kinase, respectively, by *in situ* hybridization and suggested that these genes

are involved in the development of the aposporic apomictic embryo. Silveira et al. (2012) reported the sequencing and expression analysis of expressed sequence tags (ESTs) using macroarray and reverse transcription–real-time quantitative PCR (RT-qPCR) analysis and suggested the involvement of sequences *BbrizHelic*, *BbrizRan*, *BbrizSec13*, and *BbrizSti1* in the initial steps of differentiation of the apomictic embryo sac in *U. brizantha*. Guimarães et al. (2013) found differential modulation of the MADS-box *BbrizAGL6* gene in apomictic vs. sexual *U. brizantha* genotypes.

In *U. brizantha*, Koehler et al. (2020) showed differences in the expression of the somatic embryogenesis receptor-like kinase (SERK) gene in zygotic vs. autonomous embryo development. This gene acts in somatic embryogenesis in angiosperms and is associated with apomictic processes (Podio et al., 2014). Worthington et al. (2016) developed saturated linkage maps for the maternal and paternal genomes, in addition to an interspecific *U. ruziziensis* × *U. decumbens* F1 mapping population, from which they identified molecular markers co-segregating with the apospory-specific genomic region (ASGR). In that study, the ASGR was mapped to a region of reduced recombination on chromosome 5 of *U. decumbens* (Worthington et al., 2016).

No studies have been conclusive due to the complexity of the mechanisms that trigger aposporic apomixis (Schmidt, 2020). Thus, additional studies are still needed to validate previous findings and generate new, reliable information on apomixis. Therefore, the study of candidate genes that control apomixis in *U. decumbens* may provide considerable information about the mechanisms triggering apomixis in this species and may validate previously described genes associated with this trait. This study aimed to describe the developmental stages of the embryo sac (megasporogenesis and megagametogenesis) associated with the morphometric traits of spikelets and to characterize the expression of the *BbrizRan*, *BbrizSti1*, and *BbrizAGL6* genes in *U. ruziziensis* cv. 'Kennedy' (diploid, sexual) and *U. decumbens* cv. 'Basilisk' (tetraploid, apomictic).

Material and methods

Plant material

The evaluations were performed on three clones of *U. decumbens* cv. Basilisk (apomictic, 2n = 4x = 36) and three clones of *U. ruziziensis* cv. Kennedy (sexual, 2n = 2x = 18) provided by Embrapa Gado de Leite, Juiz de Fora, Minas Gerais State, Brazil.

For morphometric evaluation of spikelets, young inflorescences were collected, fixed in Carnoy's solution, and stored at -20°C. The spikelets were excised from the racemes, and images were obtained using an image capture system (Infinity 1) coupled with a stereomicroscope (Nikon SMZ7457, Nikon instruments Inc., Melville, NY 11747-3064, U.S.A.). The length and diameter measurements of 28 spikelets were determined as the length from the pedicel to the tip of the upper glume and the maximum width of the spikelet, respectively, using ImageJ 1.51j8 software (Schindelin et al., 2015).

The spikelets were dehydrated in an ethyl alcohol series (70, 80, 90, and 100%) at −20°C and embedded in historesin using a Hydroxyethyl Methacrylate Historesin Kit (Leica, Heidelberg, Germany) following the manufacturer's instructions. The spikelets were sectioned in a semiautomatic rotary microtome Yidi YD-335 (Jinhua Yidi Medical Appliance CO., LTD, Zhejiang, China), and the sections were stained with 1% toluidine blue (O'Brien et al., 1964). Permanent slides were mounted using all-purpose varnish and evaluated under a bright-field microscope (Zeiss, model Axio Lab) equipped with an image capture system (AxioCam ERc5s). Spikelets were categorized as either megasporogenesis (ME) or megagametogenesis (MG). Spikelets undergoing ME were characterized by the arrangement of nucellar cells around the megaspore mother cell (MMC), primordial integument, and the development of the inner and outer integuments. Spikelets in MG were characterized by the presence of an enlarged functional megaspore, with vacuoles in the region of the chalazal pole, an embryonic sac of the *Polygonum* type, with eight reduced cells, two central polar nuclei, three antipodal cells, two synergids, and one oosphere.

Analysis of variance and Tukey's mean test, both at a 5% probability level, were performed using the 'agricolae' package in R version 3.6.3 (R Core Team, 2020).

Gene expression analysis

The spikelets were excised from the racemes, immediately immersed in liquid nitrogen, and stored in an ultrafreezer at −80°C. Three biological replicates of each species were collected, and each replicate consisted of a set of spikelets collected from an individual plant.

Total RNA was extracted using the PureLinkTM Plant RNA Reagent and quantified using a Nanodrop® ND-1000 Spectrophotometer. Then, the samples were treated with DNase, using Turbo DNA-free™ (Ambion) to remove residual DNA. The RNA was again quantified, and its integrity was evaluated on a 1% agarose gel with TAE buffer (Tris, acetate, and EDTA). cDNA libraries were obtained using the Applied Biosystems High Capacity cDNA Reverse Transcription Kit and stored in a −20°C freezer until analysis.

To determine the expression of candidate genes, the primers for *BbrizSti1* and *BbrizRan* were obtained from Silveira et al. (2012). For the *BbrizAGL6* gene (Guimarães et al., 2013), its sequence was initially retrieved from GenBank. To design the primers, the online resource Primer3plus (http://www.bioinformatics.nl/cgi-bin/primer3plus/primer3plus.cgi) was used, under default configuration and some adjustments, such as melting temperature (TM) - (57 a 63°C), GC content (40–60%), primer length (18–22 bp), and PCR product size (80–120 bp). Among the options suggested by the software, we chose those with lower chances of clamp and dimer formation, which was investigated by the online software OligoAnalyzer Tool (www.idtdna.com/pages/tools/oligoanalyzer).

The reference genes used in the present study, *BbrizEF1* (elongation factor-1 alpha) and *BbrizUBCE* (ubiquitin-conjugating enzyme), were the most stable in reproductive tissues and previously validated by Silveira et al. (2009) in *U. brizantha*. The *act12* (actin-12) gene was also used (Takamori et al., 2017) and selected from the database of *U. brizantha* sequences.

Primer specificity was evaluated using the melting curve, and the efficiency curve was determined using a set of all cDNA samples in five serial dilutions. Reactions were performed in 96-well optical plates in volumes of 10.0 µL sample^{-1} containing 2X SYBR Green PCR mix (Applied Biosystems), 0.2 µL of forward and reverse primers (20 pmol µL^{-1}), 1.0 µL of cDNA (5 ng µL^{-1}), and 3.6 µL of RNase and DNase-free water. The qPCR conditions were 50°C for 2 min., 95°C for 10 min., and 45 cycles of 95°C for15 s, 62°C for 30s, and 72°C for 30s. No template controls and endogenous controls were included in the analysis. Reactions were carried out in technical quadruplicates, and data were automatically generated using the 7500 Real-Time PCR system v.2.0.1 (Applied Biosystems).

The expression of the target genes *BbrizAGL6*, *BbrizSti1,* and *BbrizRan* was quantified using RT-qPCR, as previously described, with technical quadruplicates and biological triplicates. For relative quantification, the $2^{-\Delta\Delta Ct}$ comparative method was used (Pfaffl, 2001). The *BbrizEF1*, *BbrizUBCE*, and *act12* genes were used as endogenous controls for data normalization and calculated relative to a calibration sample, which was determined based on the lowest expression level for each gene.

Results and discussion

Analysis of variance (Table 1) indicated significant differences among the evaluated treatments. Considering species and developmental stage together, spikelets in ME or MG were not different between species in terms of length but rather in diameter.

Table 1. Summary of the analysis of variance of the length and diameter of the spikelets of *U. decumbens* cv. 'Basilisk' (apomictic, 2n = 4x = 36) and *U. ruziziensis* cv. 'Kennedy' (sexual, 2n = 2x = 18) in the developmental stages of megasporogenesis (ME) and megagametogenesis (MG).

Sources of variation	Length			Diameter	
	DF	MS	F value	MS	F value
Treatments	3	12.544	52.66*	1.896	32.71*
Residuals	55	0.238		0.058	

*Analysis of variance showed significant differences by the F test at 5% probability. DF: Degree of freedom; MS: Mean Square.

The spikelet length and diameter were generally greater during MG than during ME (Table 2 – part a). When analyzing these dimensions in relation to the species, some differences emerged. During MG, the spikelets of *U. ruziziensis* ranged from 5.025 to 5.891 mm in length and from 1.224 to 1.930 mm in diameter. In contrast, *U. decumbens* had spikelets measuring between 5.069 and 5.811 mm in length and between 1.532 and 2.129 mm in diameter. In both developmental stages of the embryo sac, the lengths of the spikelets from *U. ruziziensis* (5.49 mm) and *U. decumbens* (5.33 mm) were similar. However, during ME, *U. ruziziensis* spikelets ranged from 2.47 to 4.72 mm in length and from 0.56 to 1.18 mm in diameter, while those from *U. decumbens* measured between 2.77 and 4.82 mm in length and had larger diameters, ranging from 0.89 to 1.81 mm. Notably, *U. decumbens* exhibited a greater spikelet diameter (Table 2 - part b), regardless of the stage. These considerations may serve to differentiate the species in specific studies, such as this.

Table 2. Comparison of average lengths and diameters between developmental stages (megasporogenesis vs megagametogenesis), species (*U. decumbens* cv. 'Basilisk' vs *U. ruziziensis* cv 'Kennedy'), and species/stage of development (*U. ruziziensis* - megametogenesis, *U. decumbens* - megagametogenesis, *U. ruziziensis* - megasporogenesis; *U. decumbens* - megasporogenesis).

(a)	Developmental stage	Length (mm)**	Diameter (mm)**
	Megasporogenesis (ME)	3.836 b	1.183 b
	Megagametogenesis (MG)	5.438 a	1.756 a
(b)	Species/Developmental stage		
	U. ruziziensis/Megagametogenesis	5.49 a	1.68 b
	U. decumbens/Megagametogenesis	5.33 a	1.91 a
	U. ruziziensis/Megasporogenesis	4.02 b	0.97 d
	U. decumbens/Megasporogenesis	3.74 b	1.28 c

**U. decumbens* cv. Basilisk (apomictic, 2n = 4x = 36); *U. ruziziensis* cv. Kennedy (sexual, 2n = 2x = 18). **Means followed by different letters in the same column differ by Tukey's test ($p < 0.05$).

In both species, ME was characterized by the presence of nucellar cells surrounding the MMC. The MMC differs from other cells due to its larger size, vacuole, and conspicuous nucleus. As the spikelet length increased, the MMC became elongated and notably larger. This phase was also characterized by the beginning of the establishment of the primordial integument, which is found around the nucellus, in the lower part of the ovary, in the chalaza region (Figure 1a and b). The development of the internal and external integument was also observed (Figure 1).

The MG of *U. ruziziensis* was characterized by an enlarged functional megaspore with vacuoles in the chalazal pole region (Figure 1c). The histological sections of the spikelets showed an embryo sac with eight reduced cells: two polar nuclei, three antipodal cells, two synergids, and one oosphere (Figure 1d). In *U. decumbens,* the four megaspores degenerated in MG. One or more somatic cells of the nucellus were larger in size, with a prominent nucleus, a vacuole, and a thick cell wall, differing from the other cells. Such cells are called aposporous initial cells (Figure 1e). The aposporic initial cells increased in size (Figure 1e and f) and underwent two successive mitotic divisions, forming an embryo sac with four nuclei. MG was characterized by ovules with multiple (Figure 1f) and single embryo sacs (Figure 1g). In this phase, the *Panicum*-type embryo sac, typical of species with gametophytic apomixis, was composed of only four unreduced cells: one oosphere, two synergids, and one large cell containing the two polar nuclei (Figure 1g).

The integuments were fully formed in the MG stage in *U. ruziziensis* and *U. decumbens*. Nakamura et al. (2009) evaluated *Axonopus aureus* P. Beauv. and *Paspalum polyphyllum* Nees ex Trin. and reported the emergence of the inner integument before the outer integument, consisting of two to three cell layers, which divide anticlinally and periclinally, completely involving the nucellus in MG.

The MMC undergoes meiosis and originates a linear tetrad in *U. ruziziensis* (Nakamura et al., 2009), with three megaspores degenerating and one becoming functional. The functional megaspore, then, due to the formation of vacuoles, increases in volume with its nucleus positioned centrally (Nakamura et al., 2009). No dyads, tetrads, or megaspores were observed in the present study. The difficulty in selecting spikelets containing all meiosis phases suggests that this process occurs rapidly in *U. ruziziensis*.

Our results showed that the MMCs in *U. ruziziensis* and *U. decumbens* are surrounded by nucellar tissue, as already observed in *U. brizantha* (Araújo et al., 2004) and other Poaceae, such as *Olyra humilis* Nees, *Sucrea monophylla* Soderstr. (Bambusoideae), *Axonopus aureus* P. Beauv., *Paspalum polyphyllum* Nees ex Trin. (Panicoideae), *Chloris elata* Desv., and *Eragrostis solida* Nees (Chloridoideae) (Nakamura et al., 2009). The archesporial cell or MMC differs from nucellar cells in its size and evident nucleus (Nakamura et al., 2009). As meiotic division approaches, the MMC elongates, and the cytoplasm becomes dense (Nakamura et al., 2009).

For *U. ruziziensis*, the megaspore increases in size and undergoes three successive mitoses, forming an embryo sac of eight nuclei (Gobbe et al., 1982). The *Polygonum* type is composed of one or two polar nuclei in the center, in addition to three antipodals, two synergids, and one oosphere (Lituiev & Grossniklaus, 2014). In apomictic *U. decumbens*, meiosis is usually interrupted, and only one elongated meiocyte is formed. After the meiocyte degenerates, nucellar cells function as aposporic initial cells (Dusi & Willemse, 1999). The aposporic initial cells increase in size, and after two mitoses, a four-nucleus embryo sac is formed (Dusi & Willemse, 1999). In this species, an aposporic embryo sac of the *Panicum* type was confirmed, composed of the oosphere in the micropylar region, two synergids, and the central cell with a polar nucleus (Naumova et al., 1999; Araújo et al., 2004; Savidan, 2010). Oospheres in *Panicum*-type embryo sacs often have a larger size, dense cytoplasm, and a large nucleus (Naumova et al., 1999). Our evaluations in *U. decumbens* showed

one apomictic embryo sac per ovule and multiple embryo sacs per ovule, corroborating the descriptions of Naumova et al. (1999). In apomictic plants, including *U. decumbens*, one or more apomictic embryo sacs may coexist with the sexual embryo sac (Naumova et al., 1999; Araújo et al., 2000).

In *U. brizantha*, Araújo et al. (2000) compared the morphological traits of the stigma and the length of the pistil to the cytological stages of ovule formation to differentiate apomictic and sexual plants. The results obtained were important for the identification of apomictic genes in this species (Silveira et al., 2012; Guimarães et al., 2013; Lacerda et al., 2013; Ferreira et al., 2018).

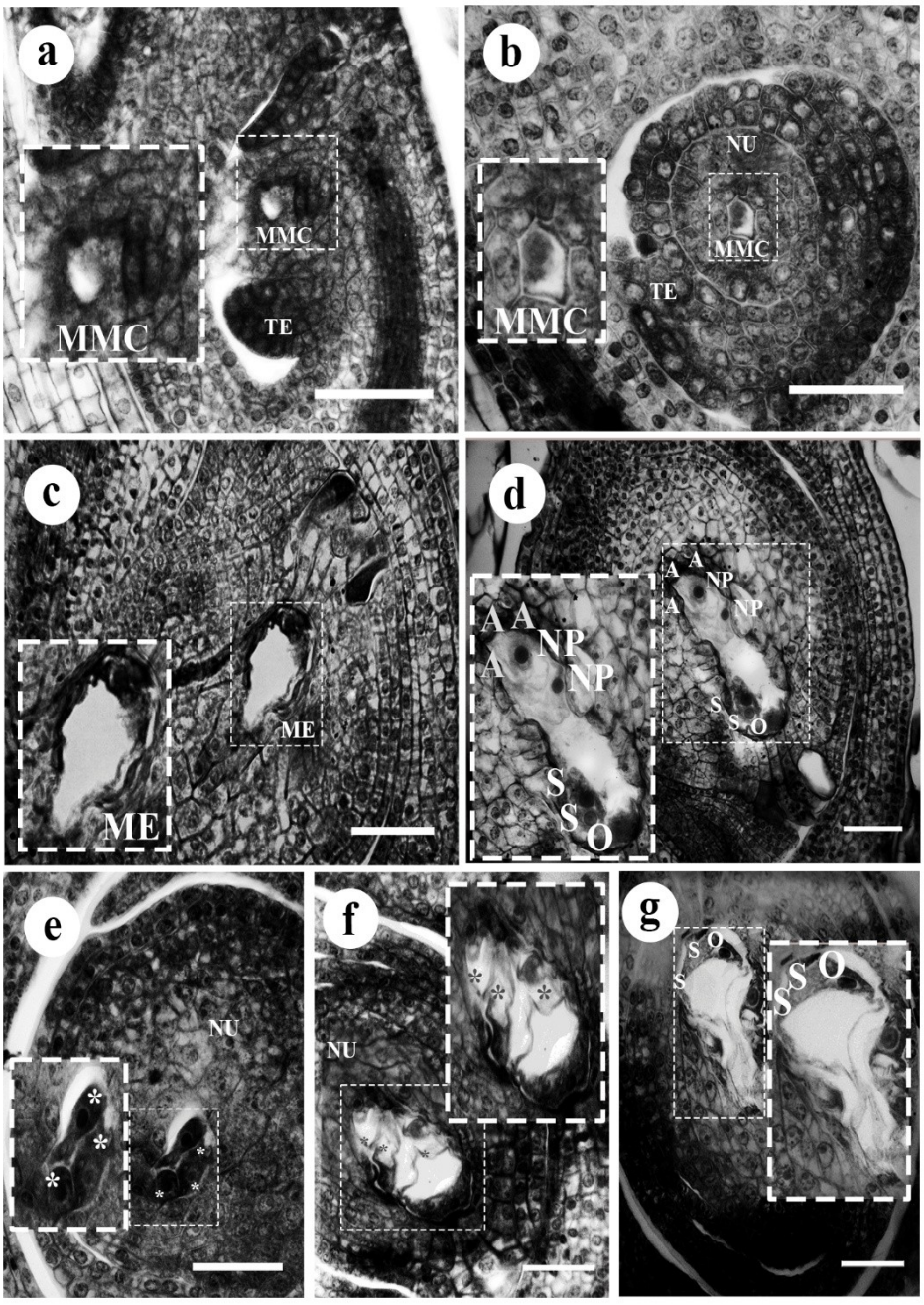

Figure 1. Megasporogenesis: a) *U. ruziziensis* cv. Kennedy (sexual) and b) *U. decumbens* cv. Basilisk (apomictic). Longitudinal sections of the spikelets show the megaspore mother cell (MMC) located in the micropylar pole, the nucellus (NU), and the primordial integument (TE). The enlarged area shows the MMC. Longitudinal section of ovaries of *U. ruziziensis* in megagametogenesis, showing c) one functional megaspore (ME), and d) the *Polygonum*-type embryo sac with eight reduced cells: two polar nuclei (NP) in the center, three antipodal cells (A), two synergids (S), one oosphere (O), and one nucellus (NU). The enlarged area shows a functional megaspore. Longitudinal section of ovaries of *U. decumbens* (apomictic) in megagametogenesis, showing e) aposporous initial cells at the beginning of differentiation from somatic cells of the nucellus (NU). The enlarged area highlights the initial aposporous cells. f) Ovary with three embryo sacs (*). The enlarged area shows the three embryo sacs. g) *Panicum*-type embryo sac composed of four unreduced cells: one oosphere (O), two synergids (S), and one cell with a polar nucleus (NP). The enlarged area shows the *Panicum*-type embryo sac. The bar represents 10 µm.

Dusi & Willemse (1999) developed a reproductive calendar for sexual and apomictic accessions of *U. decumbens* based on developmental stages of male and female gametogenesis. The authors related 11 pistil development stages that were determined from their length, morphology, days to anthesis, and the developmental stages of the female and male gametophytes. Spikelet growth accompanies the development of the embryo sac, corroborating the results of the present study. Nevertheless, our study differs by comparing ME and MG with spikelet length in *U. decumbens* cv. Basilisk and *U. ruziziensis* cv. Kennedy.

The spikelet length can be used as a reliable morphological marker to discriminate between the ME and MG stages in *U. ruziziensis* and *U. decumbens*. These results may contribute to studies that aim to characterize the expression of reproductive genes in the developmental stages of the embryo sac or to determine the mode of reproduction.

RT-qPCR analysis

The reference and target genes showed melting curves with a single peak, indicating high specificity of the primers (Figure 2). The primer amplification efficiency ranged from 84.758% (*BbrizSti1*) to 99.976% (*BbrizUBCE*) (Table 3). Confirmation of the specificity of the primers is especially important because all gene sequences evaluated were obtained from *U. brizantha* ESTs. This result suggest that the sequences of these genes show similarities between the species under study, indicating a possible common origin. Previous studies have reported high genetic proximity between the species *U. decumbens*, *U. ruziziensis*, and *U. brizantha* (Chiari et al., 2008; Paula et al., 2017). These species are part of the same agamic complex, which means that crosses can be performed between them (Renvoize et al., 1996; Chiari et al., 2008; Valle & Pagliarini, 2009; Paula et al., 2017), considering the high genetic similarity between the species observed in this study. Based on isoenzyme results, Renvoize et al. (1996) suggested that the cultivar *U. decumbens* cv. Basilisk belongs to the species *U. brizantha*.

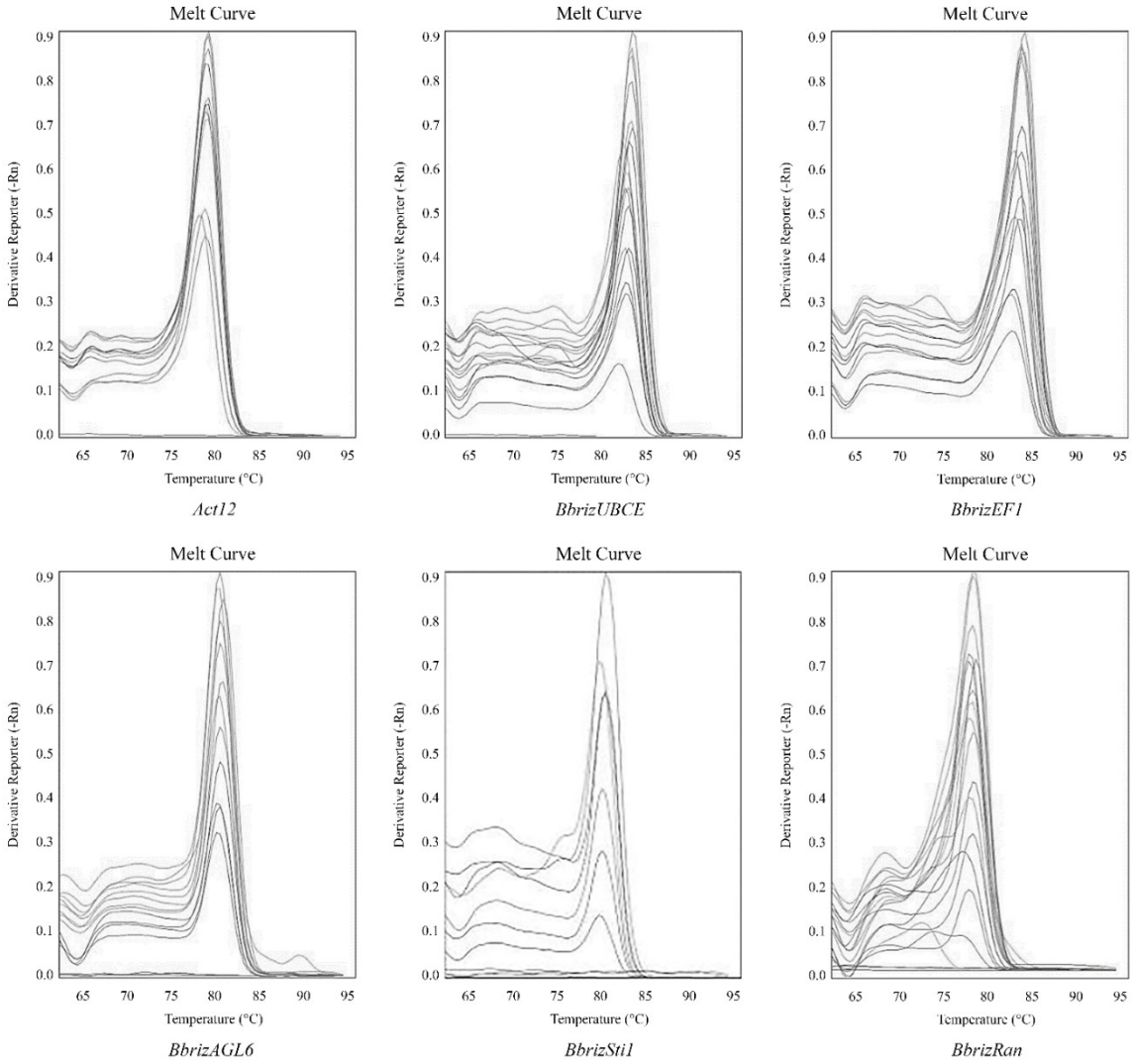

Figure 2. Melting curves of the reference genes *BbrizEF1*, *BbrizUBCE*, and act12 and target genes *BbrizAGL6*, *BbrizSti1*, and *BbrizRan*.

Table 3. Genes studied, sequence identification numbers (GenBank), primer amplification efficiencies, and forward and reverse primer pairs.

Gene	GenBank	Amplification efficiency	Forward/ Reverse Primers	Reference
BbrizSti1	JG437135	84.758	GAGCCCATAGTGGTTCATCC TCGAAAGGAGCTGGTTCAGT	Silveira et al. (2012)
BbrizRan	JG437228	95.951	CCGCCTATTTGTTCCTTGTG AAAAAGACTAGCCCCGCAAT	Silveira et al. (2012)
BbrizAGL6	JG417309	97.916	CTCACTCTGCTGCTATGGACT GCTGCGTGAATATGTTGGCTG	Guimarães et al. (2013)
BbrizEF1	EZ000623	99.165	ACCCTCCTCTTGGTCGTTTT AGCCCCTCATTTCTTCTTGG	Silveira et al. (2009)
BbrizUBCE	GE617481	99.976	GGTCTTGCTCTCCATCTGCT CGGGCTGTCGTCTCATACTT	Silveira et al. (2009)
act12	JG436709.1	96.689	GGGTGGAGAGAGATTGCAGG GGGAACTGAGGCAACCACAG	Takamori et al. (2017)

The *BbrizSti1* gene showed higher expression in the apomictic plant during ME (Figure 3a), and the *BbrizRan* gene showed higher expression in the apomictic plant during ME and MG (Figure 3b), suggesting the importance of these genes for the onset of apomictic differentiation. In MG, the expression level was high in both the sexual and apomictic species (Figure 3a and b). These genes were previously identified from EST libraries of *U. brizantha* ovaries during ME and are involved in the early stages of differentiation of the *Panicum*-type embryo sac (Silveira et al., 2012).

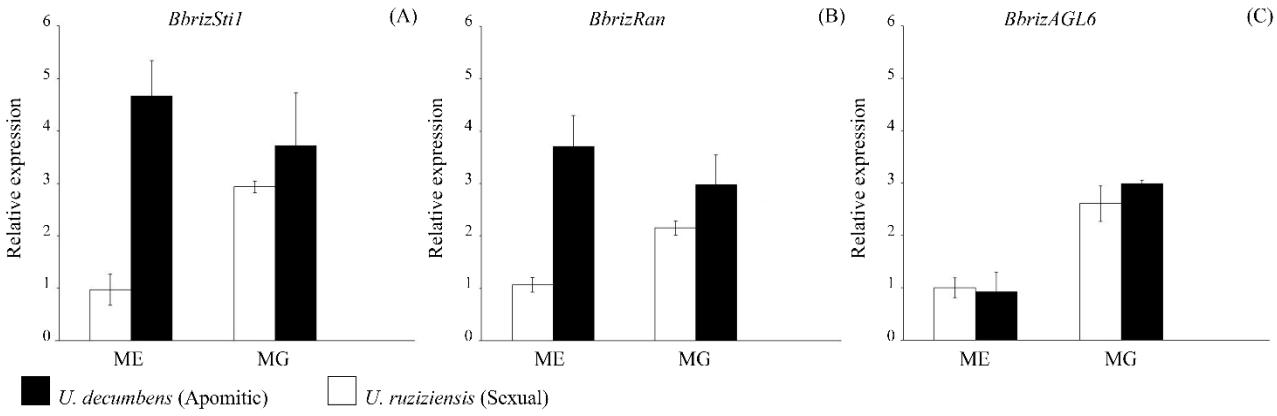

Figure 3. Relative expression of the a) *BbrizSti1*, b) *BbrizRan,* and c) *BbrizAGL6* genes in spikelets of *U. ruziziensis* cv. 'Kennedy' (sexual, 2n=2x=18) and *U. decumbens* cv. 'Basilisk' (apomictic, 2n=4x=36) during megasporogenesis (ME) and megagametogenesis (MG). The *BbrizEF1*, *BbrizUBCE*, and *act12* genes were used as reference genes (Silveira et al., 2009; Takamori et al., 2017). Bar (standard error of the mean).

BbrizSti1 is a multifunctional, stress-inducible, cochaperone protein belonging to the STI1 superfamily (Röhl et al., 2015) and found in a variety of organisms, such as fungi (Nicolet & Craig, 1989), animals (Kausar et al., 2020), and plants (Zhang et al., 2003; Lamm et al., 2017). The high expression of *BbrizSti1* in *U. decumbens* at the ME stage indicates the possible involvement of stress-responsive genes in signal transduction pathways, leading nucellar cells to act directly as aposporous initial cells (Silveira et al., 2012). Previous studies have shown the influence of different stress conditions on the expression of apomixis in plants, especially on the formation of apomictic or sexual embryo sacs, such as in weeping lovegrass (*Eragrostis curvula* [Schrad.] Nees) (Rodrigo et al., 2017) and buffel-grass (*Cenchrus ciliaris* L. [syn. *Pennisetum ciliare*]) (Gounaris et al., 1991). Studies have shown that epigenetics can control regions important for apomixis (Rodrigo et al., 2017; Fei et al., 2019).

The *BbrizRan* gene belongs to the GTP-binding nuclear protein Ran superfamily. It acts mainly in nuclear–cytoplasmic transport processes, nuclear envelope formation, and mitotic spindle formation (Boor et al., 2015). The *BbrizRan* gene in *U. decumbens* may be involved in the transport of important proteins to trigger the differentiation processes of nucellar cells into aposporous initial cells (Silveira et al., 2012).

The high levels of *BbrizSti1* and *BbrizRan* expression in both the sexual and apomictic plants at MG evaluated in our study suggest their involvement in reproductive development, possibly in mechanisms related to embryo sac formation. However, in the ovaries of sexual plants, Silveira et al. (2012) found that the *BbrizRan* gene showed

weak expression, and *BbrizSti1* was not expressed in sexual plants in any of the developmental stages, indicating that the regulation of these genes may be species-specific in the genus *Urochloa*.

BbrizSti1 expression during the development of the apomictic ovary of *U. brizantha* has been analyzed by *in situ* hybridization (Silveira et al., 2012). Signs of hybridization were detected in the ovaries in the apomictic plant from ME to MG. At the beginning of ovary development, Silveira et al. (2012) showed that *in situ* hybridization signals from the *BbrizSti1* gene were detected in MMC and surrounding nucellar cells. In the final development stage, hybridization signals were detected in integuments and nucellar cells, with weak signals in synergids, polar nuclei, and oospheres.

The *BbrizAGL6* gene was upregulated throughout embryo sac development, with peak expression in both species at MG (Figure 3c). Therefore, it is plausible to assume the participation of this gene in reproductive development. However, this result differs from that reported by Guimarães et al. (2013), in which the *BbrizAGL6* gene was differentially modulated in the ovaries of *U. brizantha*, with higher expression in the sexual genotype than in the apomictic genotype during ME and MG. In the same study, the transcripts of this gene were located in the MMC of the ovaries of apomictic and sexual plants and in the region where the aposporous initial cells differentiate in apomictic plants. These results show its presence during apomictic and sexual development, corroborating the results of the present study.

BbrizAGL6 is a gene identified in *U. brizantha* as belonging to the MIKC MADS-box family in the AGAMOUS-LIKE 6 (AGL6) subfamily (Guimarães et al., 2013). MADS-box genes link different flowering pathways (Teo et al., 2019). Reinheimer and Kellogg (2009) reported that in grasses, AGL6 genes are expressed in the ovules, lodicules, paleas, and floral meristems.

Although some studies have identified genes expressed during embryo sac formation, especially in *U. brizantha* (Alves et al., 2007; Silveira et al., 2012; Guimarães et al., 2013; Lacerda et al., 2013; Ferreira et al., 2018), the mechanisms that trigger the reproduction mode are still unknown (Fei et al., 2019; Schmidt, 2020). We verified the expression dynamics of the *BbrizRan*, *BbrizSti1*, and *BbrizAGL6* genes, suggesting a potential association with the reproductive mode of these species.

Both the use of morphometric characteristics to identify embryo sac development stages and key gene expression data complemented each other in our study and contributed to important discoveries. However, it should be noted that the need to use relatively small floral structures constituted a limiting factor (Silveira et al., 2012).

Once the differential expression of the *BbrizSti1*, *BbrizRan*, and *BbrizAGL6* genes has been detected in the different reproductive phases and species, it becomes necessary to clarify how they act and what triggers their action.

Conclusion

Spikelet length can be used as a reliable morphological marker to discriminate between MG and ME stages in *U. ruziziensis* cv. Kennedy (diploid, sexual) and *U. decumbens* cv. Basilisk (tetraploid, apomictic). The *BbrizRan*, *BbrizSti1*, and *BbrizAGL6* genes act in the reproductive development of *U. decumbens* (apomictic) and *U. ruziziensis* (sexual). The *BbrizSti1* and *BbrizRan* genes are involved in the early stages of apomictic differentiation in *U. decumbens*, and *BbrizRan* also acts in the final stages. The information obtained in this study will serve as an important tool for new studies to better understand apomixis and sexual reproduction in *Urochloa*.

Data availability

All data generated or analyzed during this study are included in this published article.

References

Albertini, E., Marconi, G., Barcaccia, G., Raggi, L., & Falcinelli, M. (2004). Isolation of candidate genes for apomixis in *Poa pratensis* L. *Plant Molecular Biology*, *56*, 879-894. https://doi.org/10.1007/s11103-004-5211-y

Alves, E. R., Carneiro, V. T. C., & Dusi, D. M. A. (2007). *In situ* localization of three cDNA sequences associated with the later stages of aposporic embryo sac development of *Brachiaria brizantha*. *Protoplasma*, *231*, 161-171. https://doi.org/10.1007/s00709-007-0253-z

Araújo, A. C. G., Mukhambetzhanov, S., Pozzobon, M. T., Santana, E. F., & Carneiro, V. T. C. (2000). Female gametophyte development in apomictic and sexual *Brachiaria brizantha* (Poaceae). *Revue de Cytologie et Biologie Végetales-Le Botaniste*, *23*, 13-26.

Araújo, A. C. G., Falcão, R., Simões, K. C. R., & Carneiro, V. T. C. (2004). *Identificação de acessos de Brachiaria com interesse ao estudo da apomixia facultativa*. Embrapa Recursos Genéticos e Biotecnologia. (Boletim de Pesquisa e Desenvolvimento, 74). https://ainfo.cnptia.embrapa.br/digital/bitstream/CENARGEN/28285/1/bp074.pdf

Chiari, L., Rocha, M., Valle, C. B., & Salgado, L. R. (2008). *Variabilidade genética em acessos e cultivares de quatro espécies de Brachiaria estimada por marcadores RAPD*. Embrapa Gado de Corte. (Boletim de Pesquisa e Desenvolvimento).

Cruz, R. P., Federizzi, L. C., & Milach, S. C. K. (1998). A apomixia no melhoramento de plantas. *Ciência Rural*, *28*(1), 155-161. https://doi.org/10.1590/S0103-84781998000100028

Boor, S., Knyphausen, P., Kuhlmann, N., Wroblowski, S., Brenig, J., Scislowski, L., Baldus, L., Nolte, H., Krüger, M., & Lammers, M. (2015). Small GTP-binding protein Ran is regulated by posttranslational lysine acetylation. *Proceedings of the National Academy of Sciences*, *112*(28), 3679-3688. https://doi.org/10.1073/pnas.1505995112

Dusi, D. M. A., & Willemse, M. T. M. (1999). Apomixis in *Brachiaria decumbens* Stapf.: Gametophytic development and reproductive calendar. *Acta Biologica Cracoviensia*, *41*, 151-162.

Fei, X., Shi, J., Liu, Y., Niu, J., & Wei, A. (2019). The steps from sexual reproduction to apomixis. *Planta*, *249*, 1715-1730. https://doi.org/10.1007/s00425-019-03113-6

Ferreira, L. G., Dusi, D. M. A., Irsigler, A. S. T., Gomes, A. C. M. M., Mendes, M. A., Colombo, L., & Carneiro, V. T. C. (2018). GID1 expression is associated with ovule development of sexual and apomictic plants. *Plant Cell Reports*, *37*, 293-306. https://doi.org/10.1007/s00299-017-2230-0

Ferreira, R. C. U., Moraes, A. C. L., Chiari, L., Simeão, R. M., Vigna, B. B. Z., & Souza, A. P. (2021). An overview of the genetics and genomics of the *Urochloa* species most commonly used in pastures. *Frontiers in Plant Science*, *12*(770461), 1-22. https://doi.org/10.3389/fpls.2021.770461

Gobbe, J., Longly, B., & Louant, B.-P. (1982). Calendrier des sporogénèses et gamétogénèses femelles chez le diploïde et le tétraploïde induit de *Brachiaria ruziziensis* (Graminée). *Canadian Journal of Botany*, *60*(10), 2032-2036. https://doi.org/10.1139/b82-250

Gounaris, E. K., Sherwood, R. T., Gounaris, I., Hamilton, R. H., & Gustine, D. L. (1991). Inorganic salts modify embryo sac development in sexual and aposporous *Cenchrus ciliaris*. *Sexual Plant Reproduction*, *4*(3), 188-192.

Guimarães, L. A., Dusi, D. M. A., Masiero, S., Resentini, F., Gomes, A. C. M. M., Silveira, É. D., Florentino, L. H., Rodrigues, J. C. M., Colombo, L. & Carneiro, V. T. C. (2013). *BbrizAGL6* is differentially expressed during embryo sac formation of apomictic and sexual *Brachiaria brizantha* plants. *Plant Molecular Biology Reporter*, *31*(6), 1397-1406. https://doi.org/10.1007/s11105-013-0618-8

Kausar, S., Abbas, M. N., Yang, L., & Cui, H. (2020). Biotic and abiotic stress induces the expression of Hsp70/90 organizing protein gene in silkworm, *Bombyx mori*. *International Journal of Biological Macromolecules*, *143*, 610-618. https://doi.org/10.1016/j.ijbiomac.2019.12.067

Koehler, A. D., Irsigler, A. S. T., Carneiro, V. T. C., Cabral, G. B., Rodrigues, J. C. M., Gomes, A. C. M. M., Togawa, R. C., Costa, M. M. C., Martinelli, A. P., & Dusi, D. M. A. (2020). SERK genes identification and expression analysis during somatic embryogenesis and sporogenesis of sexual and apomictic *Brachiaria brizantha* (Syn. *Urochloa brizantha*). *Planta, 252*(3), 39. https://doi.org/10.1007/s00425-020-03443-w

Hanna, W. W., & Bashaw, E. C. (1987). Apomixis: Its identification and use in plant breeding. *Crop Science*, *27*(6), 1136-1139. https://doi.org/10.2135/cropsci1987.0011183X002700060010x

Ishigaki, G., Gondo, T., Suenaga, K., & Akashi, R. (2009). Induction of tetraploid ruzigrass (*Brachiaria ruziziensis*) plants by colchicine treatment of *in vitro* multiple-shoot clumps and seedlings. *Grassland Science*, *55*(3), 164-170. https://doi.org/10.1111/j.1744-697X.2009.00153.x

Jank, L., Barrios, S. C., Valle, C. B., Simeão, R. M., & Alves, G. F. (2014). The value of improved pastures to Brazilian beef production. *Crop and Pasture Science*, *65*(11), 1132-1137. https://doi.org/10.1071/CP13319

Lacerda, A. L. M., Dusi, D. M. A., Alves, E. R., Rodrigues, J. C. M., Gomes, A. C. M. M., & Carneiro, V. T. C. (2013). Expression analyses of *Brachiaria brizantha* genes encoding ribosomal proteins BbrizRPS8, BbrizRPS15a, and BbrizRPL41 during development of ovaries and anthers. *Protoplasma*, *250*(2), 505-514. https://doi.org/10.1007/s00709-012-0433-3

Lamm, C. E., Kraner, M. E., Hofmann, J., Börnke, F., Mock, H.-P., & Sonnewald, U. (2017). Hop/Sti1 a two-faced cochaperone involved in pattern recognition receptor maturation and viral infection. *Frontiers in Plant Science*, *8*(1754), 1-17. https://doi.org/10.3389/fpls.2017.01754

Lituiev, D. S., & Grossniklaus, U. (2014). Patterning of the angiosperm female gametophyte through the prism of theoretical paradigms. *Biochemical Society Transactions*, *42*(2), 332-339. https://doi.org/10.1042/BST20140036

Lutts, S., Ndikumana, J., & Louant, B. P. (1991). Fertility of *Brachiaria ruziziensis* in interspecific crosses with *Brachiaria decumbens* and *Brachiaria brizantha*: meiotic behaviour, pollen viability and seed set. *Euphytica*, *57*, 267-274. https://doi.org/10.1007/BF00039673

Nakamura, A. T., Longhi-Wagner, H. M., & Scatena, V. L. (2009). Desenvolvimento de óvulo, fruto e semente de espécies de *Poaceae* (Poales). *Brazilian Journal of Botany*, *32*(1), 165-176. https://doi.org/10.1590/S0100-84042009000100016

Naumova, T. N., Hayward, M. D., & Wagenvoort, M. (1999). Apomixis and sexuality in diploid and tetraploid accessions of *Brachiaria decumbens*. *Sexual Plant Reproduction*, *12*, 43-52. https://doi.org/10.1007/s004970050170

Nicolet, C. M., & Craig, E. A. (1989). Isolation and characterization of STI1, a stress-inducible gene from *Saccharomyces cerevisiae*. *Molecular and Cellular Biology*, *9*(9), 3638-3646. https://doi.org/10.1128/mcb.9.9.3638

O'Brien, T. P., Feder, N., & McCully, M. E. (1964). Polychromatic staining of plant cell walls by toluidine blue O. *Protoplasma*, *59*, 368-373. https://doi.org/10.1007/BF01248568

Paula, C. M. P., Souza Sobrinho, F., & Techio, V. H. (2017). Genomic constitution and relationship in *Urochloa* (Poaceae) species and hybrids. *Crop Science*, *57*(5), 2605-2616. https://doi.org/10.2135/cropsci2017.05.0307

Pfaffl, M. W. (2001). A new mathematical model for relative quantification in real-time RT–PCR. *Nucleic Acids Research*, *29*(9), 2003-2007. https://doi.org/10.1093/nar/29.9.e45

Podio, M., Felitti, S. A., Siena, L. A., Delgado, L., Mancini, M., Seijo, J. G., González, A. M., Pessino, S. C., & Ortiz, J. P. A. (2014). Characterization and expression analysis of *SOMATIC EMBRYOGENESIS RECEPTOR KINASE (SERK)* genes in sexual and apomictic *Paspalum notatum*. *Plant Molecular Biology*, *84*, 479-495. https://doi.org/10.1007/s11103-013-0146-9

Reinheimer, R., & Kellogg, E. A. (2009). Evolution of AGL6-like MADS box genes in grasses (Poaceae): ovule expression is ancient and palea expression is new. *The Plant Cell*, *21*(9), 2591-2605. https://doi.org/10.1105/tpc.109.068239

Renvoize, S. A., Clayton, W. D., & Kabuye, C. H. S. (1996). Morphology, taxonomy, and natural distribution of Brachiaria (Trin.) Griseb. In J. W. Miles, B. L. Maass, C. B. Valle, & V. Kumble (Eds.), *Brachiaria: Biology, agronomy, and improvement* (pp. 1-15). CIAT.

R Core Team (2020). *R: A language and environment for statistical computing*. R Foundation for Computing. https://www.R-project.org

Rodrigo, J. M., Zappacosta, D. C., Selva, J. P., Garbus, I., Albertini, E., & Echenique, V. (2017). Apomixis frequency under stress conditions in weeping lovegrass (*Eragrostis curvula*). *PLoS ONE*, *12*(4), 1-17. https://doi.org/10.1371/journal.pone.0175852

Rodrigues, J. C., Cabral, G. B., Dusi, D. M. A., Mello, L. V., Rigden, D. J., & Carneiro, V. T. C. (2003). Identification of differentially expressed cDNA sequences in ovaries of sexual and apomictic plants of *Brachiaria brizantha*. *Plant Molecular Biology*, *53*, 745-757. https://doi.org/10.1023/B:PLAN.0000023664.21910.bd

Röhl, A., Wengler, D., Madl, T., Lagleder, S., Tippel, F., Herrmann, M., Hendrix, J., Richter, K., Hack, G., Schmid, A. B., Kessler, H., Lamb, D. C., & Buchner, J. (2015). Hsp90 regulates the dynamics of its cochaperone Sti1 and the transfer of Hsp70 between modules. *Nature Communications, 6*, 6655. https://doi.org/10.1038/ncomms7655

Sailer, C., Schmid, B., & Grossniklaus, U. (2016). Apomixis allows the transgenerational fixation of phenotypes in hybrid plants. *Current Biology*, *26*(3), 331-337. https://doi.org/10.1016/j.cub.2015.12.045

Savidan, Y. (2010). Apomixis: genetics and breeding. In *Plant breeding reviews* (v. 18, pp. 13-86). Wiley-Blackwell. https://doi.org/10.1002/9780470650158.ch2

Schindelin, J., Rueden, C. T., Hiner, M. C., & Eliceiri, K. W. (2015). The ImageJ ecosystem: an open platform for biomedical image analysis. *Molecular Reproduction and Development*, *82*(7-8), 518-529. https://doi.org/10.1002/mrd.22489

Schmidt, A. (2020). Controlling apomixis: shared features and distinct characteristics of gene regulation. *Genes*, *11*(3), 1-29. https://doi.org/10.3390/genes11030329

Silveira, É. D., Alves-Ferreira, M., Guimarães, L. A., Silva, F. R., & Carneiro, V. T. C. (2009). Selection of reference genes for quantitative real-time PCR expression studies in the apomictic and sexual grass *Brachiaria brizantha*. *BMC Plant Biology*, *9*(84), 1-10. https://doi.org/10.1186/1471-2229-9-84

Silveira, É. D., Guimarães, L. A., Dusi, D. M. A., Silva, F. R., Martins, N. F., Costa, M. M. C., Alves-Ferreira, M., & Carneiro, V. T. C. (2012). Expressed sequence-tag analysis of ovaries of *Brachiaria brizantha* reveals genes associated with the early steps of embryo sac differentiation of apomictic plants. *Plant Cell Reports*, *31*(2), 403-416. https://doi.org/10.1007/s00299-011-1175-y

Singh, M., Burson, B. L., & Finlayson, S. A. (2007). Isolation of candidate genes for apomictic development in buffelgrass (*Pennisetum ciliare*). *Plant Molecular Biology*, *64*(6), 673-682. https://doi.org/10.1007/s11103-007-9188-1

Takamori, L. M., Pereira, A. V. C., Souza, G. M., Vieira, L. G. E., & Ribas, A. F. (2017). Identification of endogenous reference genes for RT-qPCR expression analysis in *Urochloa brizantha* under abiotic stresses. *Scientific Reports*, *7*(8502), 1-11. https://doi.org/10.1038/s41598-017-09156-7

Teo, Z. W. N., Zhou, W., & Shen, L. (2019). Dissecting the function of MADS-box transcription factors in orchid reproductive development. *Frontiers in Plant Science*, *10*(1474), 1-17. https://doi.org/10.3389/fpls.2019.01474

Timbó, A. L. O., Souza, P. N. C., Pereira, R. C., Nunes, J. D., Pinto, J. E. B. P., Souza Sobrinho, F., & Davide, L. C. (2014). Obtaining tetraploid plants of ruzigrass (*Brachiaria ruziziensis*). *Revista Brasileira de Zootecnia*, *43*(3), 127-131. https://doi.org/10.1590/S1516-35982014000300004

Valle, C. B. D., Miles, J. W., Savidan, Y., Carman, J. G., & Dresselhaus, T. (2001). Breeding of apomictic species. In Y. Savidan, J. G. Carman, & T. Dresselhaus (Eds.), *The flowering of apomixis: from mechanisms to genetic engineering* (pp. 137-152). CIMMYT.

Valle, C. B. D., & Pagliarini, M. S. (2009). Biology, cytogenetics, and breeding of *Brachiaria*. In R. J. Singh (Ed.), *Genetic resources, chromosome engineering, and crop improvement series: Forage crops* (pp. 103-151). CRC Press.

Valle, C. B. D., & Savidan, Y. H. (1996). Genetics, cytogenetics, and reproductive biology of *Brachiaria*. In J. W. Miles, B. L. Maass, & C. B. D. Valle (Eds.), *Brachiaria: Biology, agronomy, and improvement* (pp. 147-163). CIAT.

Zhang, Z., Quick, M. K., Kanelakis, K. C., Gijzen, M., & Krishna, P. (2003). Characterization of a plant homolog of hop, a cochaperone of Hsp90. *Plant Physiology*, *131*(2), 525-535. https://doi.org/10.1104/pp.011940

Zorzatto, C., Chiari, L., Bitencourt, G. A., Valle, C. B., Leguizamón, G. O. C., Schuster, I., & Pagliarini, M. S. (2010). Identification of a molecular marker linked to apomixis in *Brachiaria humidicola* (Poaceae). *Plant Breeding*, *129*(6), 734-736. https://doi.org/10.1111/j.1439-0523.2010.01763.x

Worthington, M., Heffelfinger, C., Bernal, D., Quintero, C., Zapata, Y. P., Pérez, J. G., Vega, J., Miles, J., Dellaporta, S., & Tohme, J. (2016). A parthenogenesis gene candidate and evidence for segmental allopolyploidy in apomictic *Brachiaria decumbens*. *Genetics*, *203*(3), 1117-1132. https://doi.org/10.1534/genetics.116.190314